determination in humans: the lumped constant and rate constants for [^{18}F]fluorodeoxyglucose and [^{11}C]deoxyglucose. *J Cereb Blood Flow Metabol* 1985;5:179–192.
7. Martin WRW, Palmer MR, Patlak CS, Calne DB. Nigrostriatal function in humans studies with PET. *Ann Neurol* 1989;26:535–542.
8. Patlak C, Dhawan V, Takikawa S, et al. Estimation of striatal uptake rate constant of FDOPA using PET: methodologic issues. In: Uemura K, Lassen NA, Kanno I, eds. *Quantification of brain function. Tracer kinetics and image analysis in brain PET.* Amsterdam, the Netherlands: Elsevier Science Publishers; 1993:263–268.
9. Willemsem ATM, van Waarde A, Paans AMJ, et al. In vivo protein synthesis rate determination in primary or recurrent brain tumors using L-[1-^{11}C]-tyrosine and PET. *J Nucl Med* 1995;36:411–419.
10. Shields AF, Lim K, Grierson J, et al. Utilization of labeled thymidine in DNA synthesis: studies for PET. *J Nucl Med* 1990;31:337–42.
11. Mankoff DA, Shields AF, Lee TT, Graham MM. Tracer kinetic model for quantitative imaging of thymidine utilization using [^{11}C]thymidine and PET [Abstract]. *J Nucl Med* 1994;35(suppl):138P.
12. Huang S-C, Yu D-C, Barrio JR, et al. Kinetics and modeling of L-6-[^{18}F]fluoro-DOPA in human PET studies. *J Cereb Blood Flow Metab* 1991;11:898–913.
13. Vander Borght T, Labar D, Pauwels S, Lambotte L. Production of [2-^{11}C]thymidine for quantification of cellular proliferation with PET. *Appl Radiat Isotopes* 1991;42: 103–104.
14. Vander Borght T, Lambette L, Pauwels S, et al. Uptake of thymidine labeled on carbon 2: a potential indicator of liver regeneration by PET. *Hepatology* 1991;12:113–118.
15. Shields AF, Coonrod DV, Quackenbush RC, Crowley JJ. Cellular sources of thymidine nucleotides: studies for PET. *J Nucl Med* 1987;28:1435–1440.
16. Cleaver JE. Thymidine metabolism and cell kinetics. *Frontiers Biol* 1967;6:43–100.
17. Martiat P, Ferrant A, Labar D. In vivo measurement of carbon-11 thymidine uptake in non-Hodgkin's lymphoma using PET. *J Nucl Med* 1988;29:1633–1637.
18. Shields AF, Graham MM, Kozawa SM, et al. Contribution of labeled carbon dioxide to PET imaging of carbon-11-labeled compounds. *J Nucl Med* 1992;33:581–4.
19. Brooks DJ, Lammertsma AA, Beaney RP, et al. Measurement of regional cerebral pH in human subjects using continuous inhalation of [^{11}C]-CO_2 and PET. *J Cereb Blood Flow Metab* 1984;4:458–465.
20. Buxton RB, Wechsler LR, Alpert NM, et al. Measurement of brain pH using [^{11}C] CO_2 and PET. *J Cereb Blood Flow Metab* 1984;4:8–16.
21. Hetenyi Jr G, Lussier B, Ferrarotto Jr C. Calculation of the rate of gluconeogenesis from the incorporation of C-14 atoms from labeled bicarbonate or acetate. *Can J Physiol Pharmacol* 1982;60:1603–1609.
22. Johnson DC, Hoop B, Kazemi H. Movement of CO_2 and HCO_3^- from blood to brain. *J Appl Physiol* 1983;54:989–996.
23. Siesjo BK, Thompson WO. The uptake of inspired [^{14}C]-CO_2 into the acid-labile, the acid-soluble, the lipid, the protein and the nucleic acid fractions of rat brain tissue. *Acta Physiol Scand* 1965;64:182–192.
24. Lockwood AH, Finn RD. [^{11}C]-carbon dioxide fixation and equilibration in rat brain: effects on acid-base measurements. *Neurology* 1982;32:451–454.
25. Covey JM, Straw JA. Nonlinear pharmacokinetics of thymidine, thymine and fluorouracil and their kinetic interactions in dogs. *Cancer Res* 1983;43:4587–4595.
26. Goldman D, Bowen D, Gewirtz DA. Some considerations in the experimental approach to distinguishing between membrane transport and intracellular disposition of antineoplastic agents, with specific reference to fluorodeoxyuridine, actinomycin D and methotrexate. *Cancer Treatment Rep* 1981;65:43–56.
27. Kuebbing D, Werner R. A model for compartmentation of de novo and salvage thymidine nucleotide pools in mammalian cells. *Proc Natl Acad Sci* 1975;72:3333–3336.
28. Taheri MR, Wickermasingthe RG, Hoffbrand AV. Alternative metabolic fates of thymine nucleotides in human cells. *Biochem J* 1981;194:451–461.
29. Tew KD, Taylor DM. The relationship of thymidine metabolism to the use of fractional incorporation as a measure of DNA synthesis in tissue proliferation. *Eur J Cancer* 1978;14:153–168.
30. Wohlhueter RM, Marz R, Plagemann PGW. Thymidine transport in cultured mammalian cells, kinetic analysis, temperature dependence and specificity of the transport system. *Biochim Biophys Acta* 1979;553:262–283.
31. Yalowich JC, Goldman ID. Analysis of the inhibitory effects of VP-16-213 (etoposide) and podophyllotoxin on thymidine transport and metabolism in Ehrlich ascites tumor cells in vitro. *Cancer Res* 1984;44:984–989.
32. Graham MM. Parameter optimization programs for PET data analysis. *J Nucl Med* 1992;33:1069.
33. Courter JH, Link JM, Krohn KA. Automation of the synthesis of [2-carbon-11]thymidine. In: Weinrich R, ed. *Proceedings of the 4th Workshop on Targetry and Target Chemistry.* Villigen, Switzerland: Paul Scherer Institute; 1992:210–214.
34. Press W, Flannery B, Teukolsky S, Vetterling WT. *Numerical recipes in C.* New York, NY: Cambridge University Press; 1988.
35. Molnar P, Groothius D, Blasberg R, et al. Regional thymidine transport and incorporation in experimental brain and subcutaneous tumors. *J Neurochem* 1984;43: 421–432.

One-Day Protocol for Cerebral Perfusion Reserve with Acetazolamide

Naoya Hattori, Yoshiharu Yonekura, Fumiko Tanaka, Toru Fujita, Jinyi Wang, Koichi Ishizu, Hidehiko Okazawa, Nagara Tamaki and Junji Konishi

Department of Nuclear Medicine, Kyoto University, Faculty of Medicine, Kyoto; and Biomedical Imaging Research Center, Fukui Medical School, Fukui, Japan

A one-day protocol with a double injection of ^{99m}Tc-ECD was introduced for the assessment of cerebral perfusion reserve with acetazolamide (ACZ). The purpose of this study was to investigate the feasibility and effectiveness of this protocol. **Methods:** Thirty subjects were given double injections of ^{99m}Tc-ECD (first dose 370 MBq; second dose 740 MBq) for consecutive brain perfusion studies. Serial dynamic SPECT scans (1 min × 50 frames) were performed with the first set of SPECT data obtained by totaling the data for the frames taken between 5 and 20 min, and the second by subtracting the decay and dose-corrected initial SPECT data from the sum of the data obtained between 35 and 50 min. To evaluate the feasibility and effectiveness of the procedure, 23 of the 30 subjects were injected with ACZ 14 min after the first dose. To evaluate the reproducibility, seven subjects were not given the ACZ. The washout rate (WR) was calculated for three stages (WR1 = from 6 to 14 min, WR2 = from 20 to 28 min, and WR3 = from 36 to 44 min). Regional count increase (percent increase) and the percent count difference between normal and affected side (percent difference) were also calculated. **Results:** Values for WR1, WR2 and WR3 did not show significant differences among the stages (WR1 = −1.43% ± 6.09%, WR2 = −0.65% ± 6.57%, and WR3 = −1.60% ± 4.28%; F-value = 0.33, p-value = 0.72). Reproducibility was excellent (second SPECT = 0.964 × first SPECT; r = 0.997). Mean count increase after ACZ was 21.7%. In patients with unilateral cerebrovascular disease, the percent increase after ACZ loading was significantly greater on the normal side (26.6% ± 13.0%) than on the affected side (19.3% ± 13.2%) ($p < 0.01$), resulting in a significant increase in percent difference (control: 14.3% ± 10.7%, ACZ: 19.2% ± 11.5%; $p < 0.01$). **Conclusion:** ECD washout was minimal during the first 50 min after injection and was not affected by ACZ, which supports the feasibility of this protocol. The simple procedure and short acquisition time of this method renders it clinically useful for measuring cerebral perfusion reserve.

Key Words: acetazolamide; technetium-99m-ECD; double-injection protocol; cerebral perfusion reserve

J Nucl Med 1996; 37:2057–2061

Assessment of cerebral perfusion reserve in patients with an occlusive disease of the major cerebral arteries is important for the evaluation of hemodynamic compromise and candidate selection for revascularization surgery (*1–6*). Carbon dioxide or

Received Sept. 7, 1995; revision accepted Feb. 9, 1996.

For correspondence or reprints contact: Naoya Hattori, MD, Department of Nuclear Medicine, Kyoto University, Faculty of Medicine, Shogoin, Sakyo, Kyoto, 606 Japan.

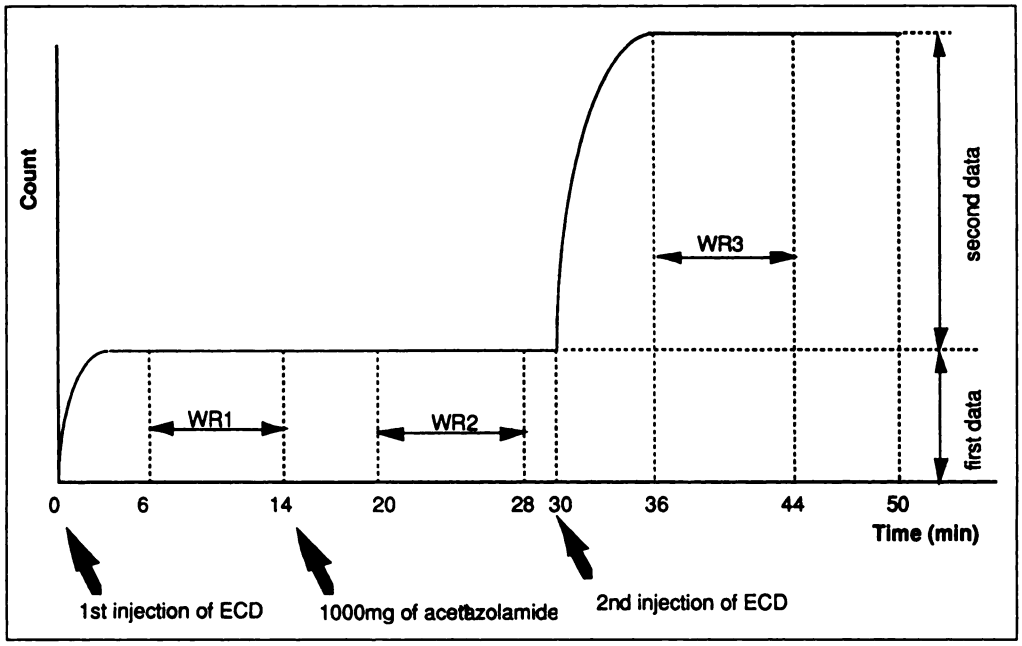

FIGURE 1. Schematic expression of the time-activity curve. X-axis is time (min); Y-axis is decay corrected regional counts. WR1 = washout rate of 6–14 min, WR2 = washout rate of 20-28 min, WR3 = washout rate of 36-44 min.

acetazolamide (ACZ) used for testing cerebral vasodilatation capacity can also demonstrate cerebral perfusion reserve in forms of an increase in regional cerebral blood flow (rCBF) (*7,8*). For this reason, various cerebral perfusion agents have been utilized in combination with ACZ. Xenon-133 and [^{123}I]IMP were found to exert superior linearity on rCBF, and found to be sensitive enough to show a 30%-70% increase of rCBF in combination with 1000 mg of ACZ in normal subjects and in the unaffected hemisphere of unilateral occlusive disease (*9,10*), however, limited availability of [^{123}I] IMP and poor spatial resolution of ^{133}Xe restrict their clinical use. Although ^{99m}Tc-hexamethylpropyleneamine (^{99m}Tc-HMPAO) has been widely used in clinical practice, ACZ loading has not been successful because of the nonlinear relationship between rCBF and regional tracer uptake, as well as poor image quality due to relatively high soft-tissue activities (*2,11*).

Technetium-99m-ethyl cysteinate dimer (ECD) provides excellent brain perfusion images with reduced soft tissue accumulation (*12,13*). The uptake of ^{99m}Tc-ECD shows significant correlation with regional cerebral blood flow (*14*) and the lesion-to-nonaffected-cortices ratio is better than for HMPAO. Moreover, the superior image quality makes it easy to interpret (*12*). This perfusion agent is also quite stable; in fact, the distribution of ^{99m}Tc-ECD did not change during a 16-hr period after injection in animals (*15–17*). It is also reported to be stable in human brain for the variety of rCBFs (*12*). If this characteristic can be maintained for 50 min and the washout rate is the same for control and under ACZ activation, consecutive brain perfusion studies performed before and after ACZ administration may accurately indicate the rCBF under both conditions by calculating the values for the ACZ loaded image. This calculation is done by simply subtracting the decay corrected control data from the data obtained after ACZ injection. The purpose of this study was to assess the feasibility of this method by measuring the washout rate and to evaluate its effectiveness for assessing cerebral perfusion reserve.

MATERIALS AND METHODS

Subjects

The study population consisted of 30 clinically symptomatic patients with suspected cerebrovascular disease. Further study revealed cerebrovascular disease in 19 patients, including unilateral and bilateral stenotic disorder in major cerebral arteries (CVD), arteriovenous fistula and cerebral aneurysm, which were all confirmed by angiography. Noninvasive studies such as SPECT, CT and MRI showed no abnormalities for the remaining 11 patients. To evaluate the feasibility and the effectiveness of the one-day ^{99m}Tc-ECD protocol, 23 patients (13 men and 10 women, age 47.0 ± 17.3 yr) underwent this protocol combined with ACZ administration at 14 min after injection (protocol A). This population included 12 patients (eight men, four women) with unilateral CVD (age 42.6 ± 19.6). To evaluate the reproducibility of the regional counts without ACZ, seven patients consisting of two men and five women (Group B: age 51.0 ± 19.8) underwent the one-day protocol without ACZ (protocol B).

SPECT Acquisition and Data Reconstruction

Serial dynamic SPECT scans (1 min × 50 frames) were obtained with a triple-head gamma camera system equipped with low-energy, high-resolution, fan-beam collimators. Two doses of ^{99m}Tc-ECD (first: approx. 370 MBq, second: approx. 740 MBq) were administered at the onset and at 30 min. In protocol A, ACZ (1000 mg) was given intravenously at 14 min (Fig. 1). Control SPECT data were obtained by totalling the data for the frames between 5 min and 20 min (first data) while the second set of SPECT data was calculated by subtraction of the first SPECT data, after decay and dose correction from the sum of the data obtained between 35 and 50 min. All data were prefiltered with a Butterworth filter (cutoff frequency of 0.4 cycle/pixel, power factor 4.0) followed by reconstruction using a filtered backprojection algorithm with a ramp filter, and display on a 64 × 64 matrix. The pixel size was 3.4 × 3.4 mm, and the slice thickness was 7.1 mm. Attenuation correction with Chang's method was performed for each slice with a uniform attenuation coefficient of 0.09/cm, which was determined by the uniform cylindrical phantom in 16 cm diameter in order to obtain the uniform activity.

Data Analysis

To locate regions of interest (ROIs), a standard slice at the lateral ventricular level was selected from the transverse image set. A pair of ROIs were then manually located on the slice to include both right and left cerebral cortices for every patient. In protocol A, 12 ROIs were placed over the affected cortices. To calculate the washout rate, the regional counts of every frame was decay corrected. The washout rate (WR) was calculated for three stages

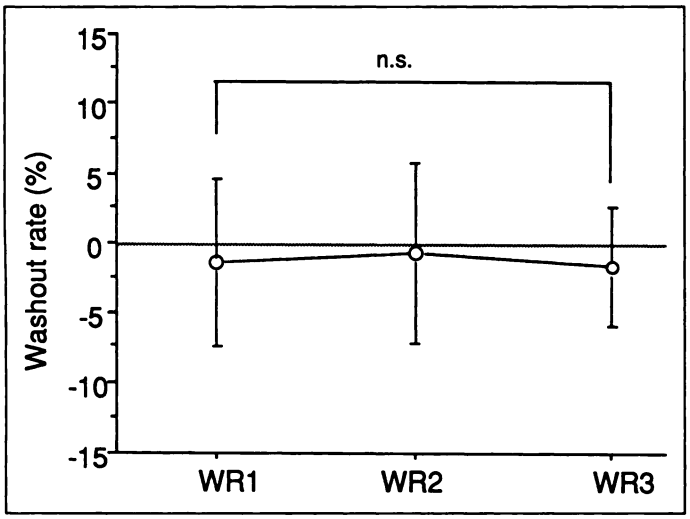

FIGURE 2. Changes of washout rate before (WR1) and after ACZ loading (WR2, WR3). There were no significant changes among three stages. WR1 = washout rate of 6–14 min, WR2 = washout rate of 20–28 min, WR3 = washout rate of 36–44 min.

(WR1 = from 6 to 14 min, WR2 = from 20 to 28 min, and WR3 = from 36 to 44 min) (Fig. 1) to analyze the WR under control conditions, under ACZ activation, and under activation after the second injection. Thus, the following formulas were used:

$$WR1 = \frac{(\text{counts at 6 min} - \text{counts at 14 min})}{\text{counts at 6 min}} \times 100\,(\%)\,; \quad \text{Eq. 18}$$

$$WR2 = \frac{(\text{counts at 20 min} - \text{counts at 28 min})}{\text{counts at 20 min}} \times 100\,(\%)\,; \quad \text{Eq. 19}$$

$$WR3 = \frac{(\text{counts at 36 min} - \text{counts at 44 min})}{\text{counts at 36 min}} \times 100\,(\%)\,. \quad \text{Eq. 20}$$

To compare the differences in regional count increases, under ACZ activation on the normal and affected side of unilateral CVD in protocol A, and to calculate the reproducibility of the regional counts without ACZ in protocol B, dose corrected regional counts for the first set of data (Ct1 = first counts/first dose) and the second set (Ct2 = second counts/second dose) were compared.

In patients with unilateral CVD, the regional count increase after normalization of the injected dose (% increase, Fig. 1), and the percent count difference between normal and affected sides (% difference) were also calculated as follows:

TABLE 1
Washout Rate Summary

Stages	Patients with unilateral CVD: Normal side (12 ROIs)	Patients with unilateral CVD: Affected side (12ROIs)	Significance of difference (t-value/p-value)	All subjects Overall (46 ROIs)
WR1	−3.77 ± 4.74	0.14 ± 5.24	n.s. (−1.88/0.09)	−1.43 ± 6.09
WR2	−0.43 ± 5.22	−2.38 ± 7.53	n.s. (0.69/0.50)	−0.65 ± 6.57
WR3	−1.05 ± 2.31	−1.76 ± 5.40	n.s. (0.38/0.71)	−1.60 ± 4.28

Data are expressed as mean ± s.d. (%/hr). n.s. = not significant.
Difference between normal side and affected side were analyzed using paired t-test.

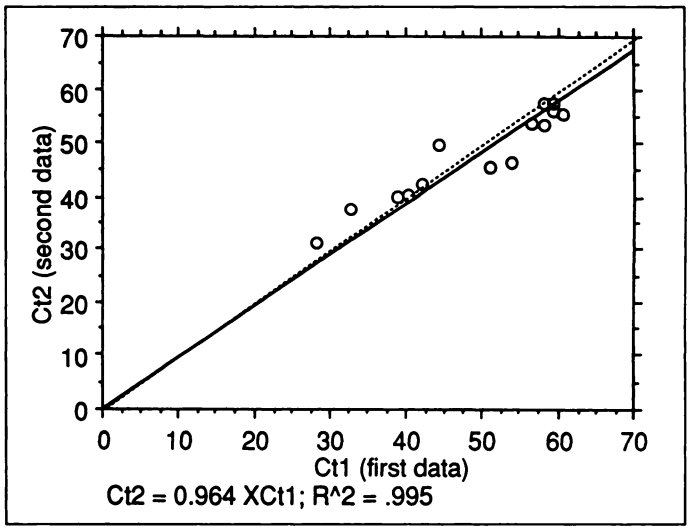

FIGURE 3. Dose-corrected regional counts of first data (Ct1 = first counts/first dose) and second data (Ct2 = second counts/second dose) were compared. Without ACZ, the reproducibility was excellent (Ct2 = 0.964 × Ct1, r = 0.997). Dotted line: line of identity.

$$\%\text{increase} = \frac{(Ct2 - Ct1)}{Ct1} \times 100\,(\%)\,; \quad \text{Eq. 21}$$

$$\%\text{difference} = \frac{(\text{counts on the normal side} - \text{counts on the affected side})}{\text{counts on the normal side}} \times 100\,(\%)\,. \quad \text{Eq. 22}$$

Statistical Analysis

Data were expressed as mean ± s.d. Changes in the WR for the three stages were analyzed by ANOVA with repeated measurements. Regression analysis was performed to compare the regional counts of the first and the second set of data. Differences in the WR and percent increase between the normal and affected side, and changes in the percent difference after ACZ loading were analyzed

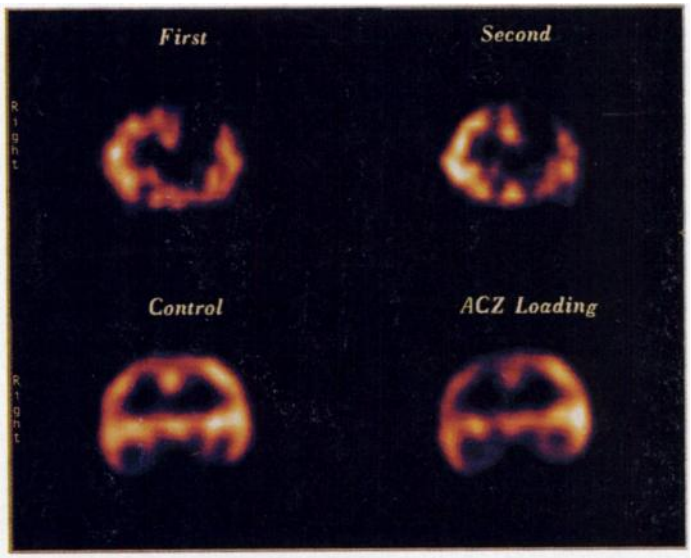

FIGURE 4. Top: Images from a subject in protocol B to demonstrate the reproducibility. Representative slices of the first (left) and second (right) SPECT images showed almost identical cerebral perfusion images. Bottom: Images from a subject in protocol A to demonstrate the difference of percent increase between the normal and affected sides. ACZ activation SPECT (right) showed reduced cerebral perfusion reserve in the right side (percent increase: 15.1% in the right, 22.9% in the left) compared with a SPECT image of control condition (left).

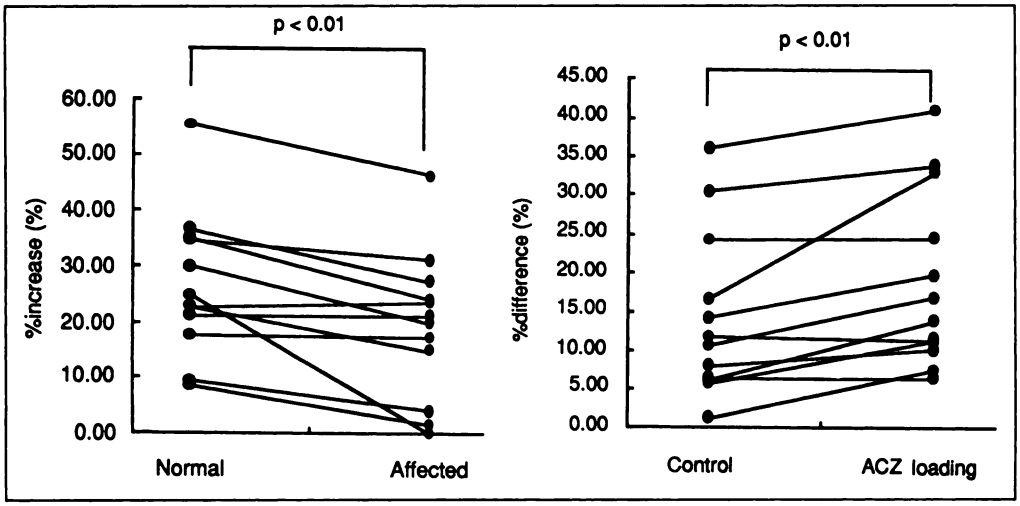

FIGURE 5. Left: Difference of percent increase after ACZ loading. Percent increase of the normal sides was significantly larger than that of the affected sides ($p < 0.01$). Right: %difference between the normal and the affected sides before and after ACZ loading. The %difference significantly increased after ACZ loading ($p < 0.01$).

with the paired t-test. The difference was considered to be significant if the p value was less than 5% ($p < 0.05$).

RESULTS

Washout Rate

In protocol A, a total of 46 ROIs were analyzed. The washout rate of ^{99m}Tc- ECD from 6 to 14 min (WR1) was $-1.43 \pm 6.09\%$, from 20 to 28 min (WR2) was $-0.65 \pm 6.57\%$, and from 36 to 44 min (WR3) was $-1.60 \pm 4.28\%$. Although WR1 and WR3 were lower than WR2 (Fig. 2), the difference was not significant (F-value = 0.33, p-value = 0.72) (Table 1). For 12 patients with unilateral CVD, a comparison of the difference in washout rate between normal and affected side showed no significant difference between the two sides for any stage (t-value/p-value were −1.88/0.09 in WR1, 0.69/0.50 in WR2 and 0.38/0.71 in WR3) (Table 1).

Reproducibility

In protocol B, a total of 14 ROIs were studied. The reproducibility of the dose corrected first regional counts (Ct1) and the second regional counts (Ct2) was excellent ($Ct2 = 0.964 \times Ct1$, $r = 0.997$). Only 3.6% of the regional counts was underestimated for the second set of data (Figs. 3, 4).

Effect of ACZ

The mean regional count increase after ACZ administration in patients with unilateral CVD (24 ROIs) showed a 21.7% of count increase after ACZ administration ($Ct2 = 1.217 \times Ct1$).

To evaluate the effectiveness of this protocol, the percent increase between the normal and affected side and the percent difference before and after ACZ injection were calculated for this group (12 ROIs on the normal side versus 12 ROIs on the affected side). The percent increase after ACZ loading was significantly greater on the normal side ($26.6\% \pm 13.0\%$) than on the affected side ($19.3\% \pm 13.2\%$) (t-value = 3.71/ p-value < 0.01), resulting in a significant increase in percent difference between the normal and the affected side (control: $14.3 \pm 10.7\%$, loading: $19.2 \pm 11.5\%$; t-value = −3.69/ p-value < 0.01) (Figs. 4, 5).

DISCUSSION

In present study, the WR of ^{99m}Tc-ECD was minimal during the initial 50-min period and was not affected by ACZ, while reproducibility of the first and second sets of data was excellent for this one-day protocol, thus, demonstrating the feasibility of this method. It also verifies the validity of quantitative assessment of perfusion reserve with this protocol, by showing a significant difference in count increase after ACZ loading between the normal and affected side. The data also serve to validate visual assessment of reduced perfusion reserve by this method because the percent difference increased after ACZ loading.

Feasibility of One-Day Protocol

The basic purpose of the one-day protocol is to perform consecutive brain perfusion studies before and after ACZ administration, and achieved by calculating the ACZ loading image through simply subtracting the decay-corrected control data from the data obtained after ACZ injection, and by assuming that there is no washout of the radiotracer from the brain. Therefore, validation of this method requires the following conditions: (a) WR of ^{99m}Tc-ECD should be neglectable, even after the increase in the cerebral blood flow due to ACZ administration (WR2 = 0); and (b) washout of control data and second data should be almost equal (WR1 = WR3).

WR1 (6–14 min) represents the washout rate for rCBF under control conditions, because ACZ was injected at 14 min. WR2 is considered to represent the WR of the first dose during the activation, because CBF increases approximately 5 min after ACZ injection, and the effect lasts more than 40 min (*9,18*). Finally, WR3 represents the total washout of the first and second tissue counts.

Our results showed no significant differences among WR1,WR2 and WR3. WR2 was negligible (−0.65%), and smaller than that reported in several previous studies (*12–15,19*). There is, however, agreement in that there was almost no washout of ^{99m}Tc-ECD from the brain. The excellent reproducibility of the regional counts without ACZ administration also supports the feasibility of this method. The second regional counts was underestimated by only 3.6%, which is almost same as the value reported for HMPAO (*20*).

Advantages and Disadvantages of Technetium-99m-ECD One-Day Protocol

Use of protocol with ^{99m}Tc-ECD resulted in a percentage increase after ACZ administration of $26.6\% \pm 13.0\%$ on the normal and $19.3\% \pm 13.2\%$ on the affected sides. The contrast between the two sides (percent difference) increased from $14.3\% \pm 10.7\%$ to $19.2\% \pm 11.5\%$. This percent increase was smaller than the values reported for ^{133}Xe (*9*) or [^{123}I]IMP (*10*), but larger than that for HMPAO (*20*).

The major disadvantage of using ^{99m}Tc-ECD is that it leads to underestimation of the increase in rCBF. As we proved in this study, ^{99m}Tc-ECD washout from the brain was minimal; therefore, the underestimation is probably caused by the nonlinear relationship between ^{99m}Tc-ECD uptake and regional CBF due

to the limited extraction of ^{99m}Tc-ECD (below 70%) (*21,22*). Some sort of correction may thus be required to obtain the true increase in regional CBF. Iodine-123-IMP, however, is inconvenient for routine studies because of its limited commercial supply. Moreover, this tracer redistributes over time in conjugation with the flow dependent washout from the brain, which is not ideal for an ACZ loading study (*23,24*). Xenon-133 requires special equipment for SPECT measurement, and its poor spatial resolution restricts the detailed assessment of regional CBF changes. Compared with HMPAO, ECD showed a greater percent increase suggesting less underestimation of rCBF. HMPAO yields greater extraction than ^{99m}Tc-ECD, but initial backdiffusion is prominent, resulting in a smaller percent increase in the tissue counts (*25*).

As we and other authors have reported, ^{99m}Tc-ECD distribution is stable over time, and its washout is independent from rCBF (*12,15,17*). This is an important characteristic for assessing rCBF changes before and after ACZ administration. It should also be noted that the image quality of ^{99m}Tc-ECD is excellent, because of less background accumulation, thus making the image easier to interpret (*12,13,15*).

Future Implications

The ultimate goal of this study is to establish the ultra-short one-day protocol. For this purpose it is possible to omit the WR1 phase from our study design. By taking the first (control) and second (control+loading) scans at intervals of 15 min and injecting ACZ at 5 min, the control and loading images could be obtained in only 35 min. The scanning time may also be shortened, depending on the facilities, so that it may be possible to complete the one-day protocol within 35 min.

This method is also applicable to activation studies other than for ACZ loading. One major advantage of the one-day protocol is the ease of patient positioning, because the short scanning time makes it easier for the patients to stay in bed without moving during the study. The activated area is visualized by simply subtracting data for the first scan from those for the second scan after dose and decay correction.

CONCLUSION

Double injection of ^{99m}Tc-ECD and the subtraction method was validated by examining the washout rate during a 50-min period. The WR of ^{99m}Tc-ECD was minimal during this period and CBF did not increase as a result of ACZ administration. With its superior image quality and ease of imaging protocol, this method should be clinically useful for various activation studies using SPECT.

ACKNOWLEDGMENTS

We thank Drs. S. Miyamoto, M. Tanaka and I. Nakahara (Department of Neurosurgery) for their cooperation in providing clinical information on the patients, and H. Kitano, BS for technical assistance. This work was presented in part at the 42nd Annual Meeting of the Society of Nuclear Medicine, Minneapolis, June 1995.

REFERENCES

1. Dingler WH, Deininger HK. The value of the acetazolamide stimulation test with ^{99m}Tc-HMPAO SPECT in reversible cerebrovascular insufficiency. *Rofo Fortschr Geb Rontgenstr Neuen Bildgeb Verfahr* 1991;155:465–71.
2. Knop J, Thie A, Fuchs C, Siepmann G, Zeumer H. Technetium-99m-HMPAO SPECT with acetazolamide challenge to detect hemodynamic compromise in occlusive cerebrovascular disease. *Stroke* 1992;23:1733–1742.
3. Ramsay SC, Yeates MG, Lord RS, et al. Use of technetium-99m-HMPAO to demonstrate changes in cerebral blood flow reserve following carotid endarterectomy. *J Nucl Med* 1991;32:1382–1386.
4. Shinoda J, Kimura T, Funakoshi T, Araki Y, Imao Y. Acetazolamide reactivity on cerebral blood flow in patients with subarachnoid haemorrhage. *Acta Neurochir Wien* 1991;109:102–108.
5. Mountz JM, Deutsch G, Khan SH. Regional cerebral blood flow changes in stroke imaged by technetium-99m-HMPAO SPECT with corresponding anatomic image comparison. *Clin Nucl Med* 1993;18:1067–1082.
6. Lassen NA. Pathophysiology of brain ischemia as it relates to the therapy of acute ischemic stroke. *Clin Neuropharmacol* 1990;13:S1–S8.
7. Adams JM, Johnson NL. Inhibiting carbonic anhydrase in brain tissue increases the respiratory response to rebreathing CO_2. *Brain Res* 1990;519:23–28.
8. Hanson MA, Nye PC, Torrance RW. The location of carbonic anhydrase in relation to the blood-brain barrier at the medullary chemoreceptors of the cat. *J Physiol Lond* 1981;320:113–125.
9. Vorstrup S, Henriksen L, Paulson OB. Effect of acetazolamide on cerebral blood flow and cerebral metabolic rate for oxygen. *J Clin Invest* 1984;74:1634–1639.
10. Nishizawa S, Yonekura Y, Tanaka F, et al. Evaluation of a double-injection method for sequential measurement of cerebral blood flow with iodine-123-iodoamphetamine. *J Nucl Med* 1995;36:1339–1345.
11. Burt RW, Witt RM, Cikrit D, Carter J. Increased brain retention of technetium-99m-HMPAO following acetazolamide administration. *Clin Nucl Med* 1991;16: 568–571.
12. Leveille J, Demonceau G, Walovitch RC. Intrasubject comparison between technetium-99m-ECD and technetium-99m-HMPAO in healthy human subjects. *J Nucl Med* 1992;33:480–484.
13. Walovitch RC, Franceschi M, Picard M, et al. Metabolism of ^{99m}Tc-L,L-ethyl cysteinate dimer in healthy volunteers. *Neuropharmacology* 1991;30:283–292.
14. Devous M, Sr, Payne JK, Lowe JL, Leroy RF. Comparison of technetium-99m-ECD to xenon-133 SPECT in normal controls and in patients with mild- to-moderate regional cerebral blood flow abnormalities. *J Nucl Med* 1993;34:754–761.
15. Leveille J, Demonceau G, De-Roo M, et al. Characterization of technetium-99m-L,L-ECD for brain perfusion imaging: part 2. Biodistribution and brain imaging in humans. *J Nucl Med* 1989;30:1902–1910.
16. Greenberg JH, Lassen NA. Characterization of ^{99m}Tc-bicisate as an agent for the measurement of cerebral blood flow with SPECT. *J Cereb Blood Flow Metab* 1994;14:S1–S3.
17. Walovitch RC, Hill TC, Garrity ST, et al. Characterization of technetium-99m-L,L-ECD for brain perfusion imaging: part 1. Pharmacology of technetium-99m-ECD in nonhuman primates. *J Nucl Med* 1989;30:1892–1901.
18. Hauge A, Nicolaysen G, Thoresen M. Acute effects of acetazolamide on cerebral blood flow in man. *Acta Physiol Scand* 1983;117:233–239.
19. Friberg L, Andersen AR, Lassen NA, Holm S, Dam M. Retention of ^{99m}Tc-bicisate in the human brain after intracarotid injection. *J Cereb Blood Flow Metab* 1994;14:S19–S27.
20. Matsuda H, Higashi S, Kinuya K, et al. SPECT evaluation of brain perfusion reserve by the acetazolamide test using technetium-99m-HMPAO. *Clin Nucl Med* 1991;16:572–579.
21. Tsuchida T, Nishizawa S, Yonekura Y, et al. SPECT images of technetium-99m-ethyl cysteinate dimer in cerebrovascular diseases: comparison with other cerebral perfusion tracers and PET. *J Nucl Med* 1994;35:27–31.
22. Di-Rocco RJ, Silva DA, Kuczynski BL, et al. The single-pass cerebral extraction and capillary permeability-surface area product of several putative cerebral blood flow imaging agents. *J Nucl Med* 1993;34:641–648.
23. Creutzig H, Schober O, Gielow P, et al. Cerebral dynamics of N-isopropyl-(^{123}I)p-iodoamphetamine. *J Nucl Med* 1986;27:178–183.
24. Lassen NA, Henriksen L, Holm S, et al. Cerebral blood-flow tomography: xenon-133 compared with isopropyl-amphetamine-iodine-123: concise communication. *J Nucl Med* 1983;24:17–21.
25. Murase K, Tanada S, Fujita H, Sakaki S, Hamamoto K. Kinetic behavior of technetium-99m-HMPAO in the human brain and quantification of cerebral blood flow using dynamic SPECT. *J Nucl Med* 1992;33:135–143.